Columnar Growth in Thin Films

A. Mazor,(1) D. J. Srolovitz,(1,2) P. S. Hagan,(1) and B. G. Bukiet(1)
(1)*Theoretical Division, Los Alamos National Laboratory, Los Alamos, New Mexico 87545*
(2)*Department of Materials Science and Engineering, University of Michigan, Ann Arbor, Michigan 48109*

(Received 21 September 1987)

A theory for the growth of columnar microstructures in thin films is presented. The zone-I to zone-II transition temperature is predicted. The surface morphology and the columnar grain structure are obtained both analytically and numerically, and the scaling behavior of the columnar grain size with film thickness is derived. Monte Carlo simulations are used to follow the evolution of the three-dimensional zone-II microstructures and to account for the formation of film texture. These results agree with experimental observations.

PACS numbers: 68.55.Jk, 68.55.Ce, 81.10.Bk

Over the last two decades a detailed experimental classification of thin-film morphology has been made.[1-3] The technological importance of such studies arises from the relation between the physical structure of thin films and desired film properties. Depending on the material and the preparation parameters, high-rate vapor-deposited films are finding increasing applications as coatings with high corrosion resistance, high hardness, controlled porosity, etc.[4]

The microstructure of vapor-deposited films depends sensitively on deposition conditions, among which the substrate temperature T is of particular importance. For high deposition rates (how high depends on the material, but 10000 to 250000 Å min^{-1} are typical[2]) three temperature zones have been identified, each of which is characterized by a distinct type of microstructure.[1,2] For $0<T<T_1$ (where $T_1 \simeq 0.3T_m$ for metals, $\simeq 0.24T_m$ for oxides, and T_m is the melting temperature of the film), the microstructure is porous and suggests ballistic aggregation. For $T_1<T<T_2$, where $T_2 \simeq 0.45T_m$, the film consists of columnar grains separated by metallurgical grain boundaries. For $T_2<T<T_m$, the structure is that of equiaxial grains. These different microstructural regimes are known as zones I, II, and III, respectively.

The current state of understanding the deposition-condition dependence of high-rate deposited film microstructure is based on a great body of experimental experience, but has suffered from lack of theoretical insight and guidance. This Letter represents one of the first ventures in this area. We present both a theoretical model and numerical results which show that the columnar zone-II microstructures are primarily controlled by the competition between a growth instability inherent in the deposition of finite-size atoms and the stabilizing influence of surface diffusion. One of the prime novelties of this work is the consequences of the combination of both these effects in their nonlinear form in the following evolution equation for the film surface. The solution of Eq. (1) below sheds a great deal of light on the mechanisms governing the formation and evolution of film morphology and microstructure as a function of deposition conditions. This model quantitatively describes the zone-I to zone-II transition temperature, the surface morphology, the columnar grain structure, the dependence of the grain size on film thickness, and the development of film texture, closely matching the experimental observations.

With the assumptions of a constant uniform deposition rate J of atoms of radius δ, and a finite surface diffusivity (see Fig. 1), the evolution of the one-dimensional surface profile $h(x,t)$ is given by

$$h_t = J - \delta J h_{xx}(1+h_x^2)^{-3/2} - D_e\{(1+h_x^2)^{-1/2}[h_{xx}(1+h_x^2)^{-3/2}]_x\}_x. \quad (1)$$

Here $D_e = D_s \sigma_s \Omega^2 \epsilon / K_B T$, where D_s is the surface diffusivity, σ_s the isotropic surface energy density, Ω the atomic volume, ϵ the number of atoms per unit area, and $K_B T$ the thermal energy. We now briefly outline the derivation of (1) (more details will be presented elsewhere[5]). The first two terms on the right-hand side (rhs) of (1) constitute the nonlinear version of the finite

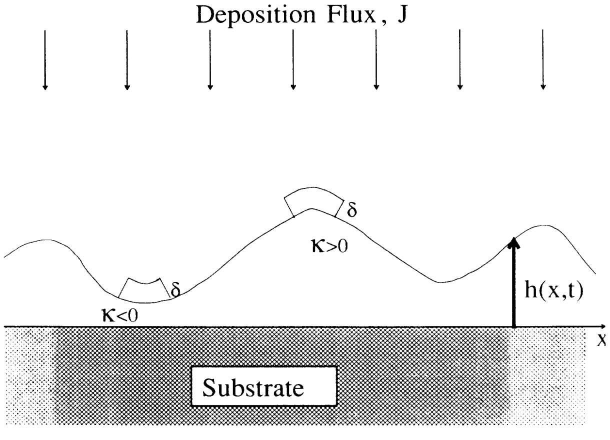

FIG. 1. The deposition geometry (κ is the surface curvature).

© 1988 The American Physical Society

atomic size effect discussed by Leamy, Gilmer, and Dirks.[6] Since $\delta \neq 0$, the deposition actually takes place on an imaginary surface displaced by $\delta \mathbf{n}(x)$ from $h(x)$ [$\mathbf{n}(x)$ is a unit vector normal to $h(x)$]. The projection of an element of $h(x)$ on the x axis is varied because of the above displacement. This variation multiplied by J is the local growth rate of the surface, given (to leading order in δ) by the first two terms on the rhs of (1). Thus an element of the surface $h(x,t)$ receives a net flux of atoms greater (for positive surface curvature $\kappa > 0$) or smaller (for $\kappa < 0$) than J. The last term in (1) describes relaxation of the surface by a capillarity-driven surface diffusion. This effect has been suggested by Mullins[7] through numerous studies. Since the chemical potential μ of an atom on a curved surface is raised by $\sigma_s \Omega \kappa$ over that of a flat profile, the velocity of atoms along the surface is $v_s = -(D_s/K_B T)\partial\mu/\partial s$ (s is an element of arc along the surface). Thus the velocity of the surface normal to itself (due to surface diffusion) is $-\Omega\partial(\epsilon v_s)/\partial s$, where ϵv_s is the surface current of atoms.

Linearization of (1) about a flat surface shows that an initial trial sinusoidal perturbation $\sin(kx)$ grows or decays according to $\exp[(\delta J k^2 - D_e k^4)t]$ for short times. Thus a band of unstable modes exists with wavelengths $\lambda = 2\pi/k > \lambda_0 = (4\pi^2 D_e/\delta J)^{1/2}$, and with the most unstable mode at $\lambda = \lambda_m \equiv \sqrt{2}\lambda_0$. Perturbations with wavelengths smaller than the diffusion length $\lambda_0(T)$ are smoothed by surface diffusion, whereas long-wavelength perturbations grow unstably. As a result of the discrete nature of the atoms in the film, surface diffusion is ineffective when the diffusion length $\lambda_0(T)$ is smaller than a few times δ. Equating $\lambda_0(T)$ with the minimum physically meaningful diffusion length $\eta\delta$ (where η is a constant of order 1 to 10) yields a critical temperature below which surface diffusion plays essentially no role in the microstructural evolution. If we substitute $\sigma_s = 10^3$ dyn/cm, $\Omega = 2\times10^{-23}$ cm^3, $\delta = 4\times10^{-8}$ cm, $J = 2\times10^{-5}$ cm/sec, and $\eta = 5$, the equality $\lambda_0(T) = \eta\delta$ is satisfied at $T = T_c \approx 0.23 T_m$. Since D_e is proportional to D_s, which depends exponentially on temperature[8] [i.e., $D_s = D_0 \exp(-Q/K_B T)$, where $Q = (5 + 20T/3T_m) \times K_B T_m$], T_c is relatively insensitive to variations around 5δ. Since the zone-I film microstructure is of the form produced by ballistic aggregation (i.e., the zero-diffusion limit), we equate T_c with T_1. The calculated value of T_1 is in good agreement with the experimental value.

The nonlinear terms in (1) saturate the long-wavelength instability into a relatively small-amplitude columnar surface profile. The free-energy formalism[9] shows that the steady-state solutions of the full nonlinear, partial differential growth equation (1) are described by

$$H^2 - (1 + H_z^2)^{-1/2} = C, \tag{2}$$

where C, $-1 < C < \infty$, is an integration constant; $H = (\delta J/2D_e)^{1/2}(h - Jt)$; and $z = (\delta J/2D_e)^{1/2}x$. Solving (2) for $-1 < C < 0$ yields the roughly sinusoidal steady-state surface profiles

$$H = (1 + C)^{1/2}\cos a(z), \tag{3}$$

where

$$2E(a,r) - F(a,r) = z\sqrt{2} + \text{const}, \quad r = [(1+C)/2]^{1/2},$$

and E and F are incomplete elliptic integrals. When $C > 0$, the solution of (2) is still given by (3) until $\sin^2 a$ reaches $1/(1+C)$; the solution then jumps from $H = +C$ to $H = -C$ (or from $H = -C$ to $H = +C$) and then (3) again pertains. Thus the steady-state profiles with $C > 0$ consist of very nearly circular arcs connected by vertical lines. Both the characteristic wavelength of these profiles and their amplitude decrease monotonically as C increases. The value of C is determined by the maximally unstable mode (assuming small-amplitude initial condition). These steady states have been shown numerically to be stable with respect to small perturbations.[5]

In order to demonstrate that the solutions (3) with $C > 0$ are stable steady states which can be reached from typical initial conditions, we have integrated (1) numeri-

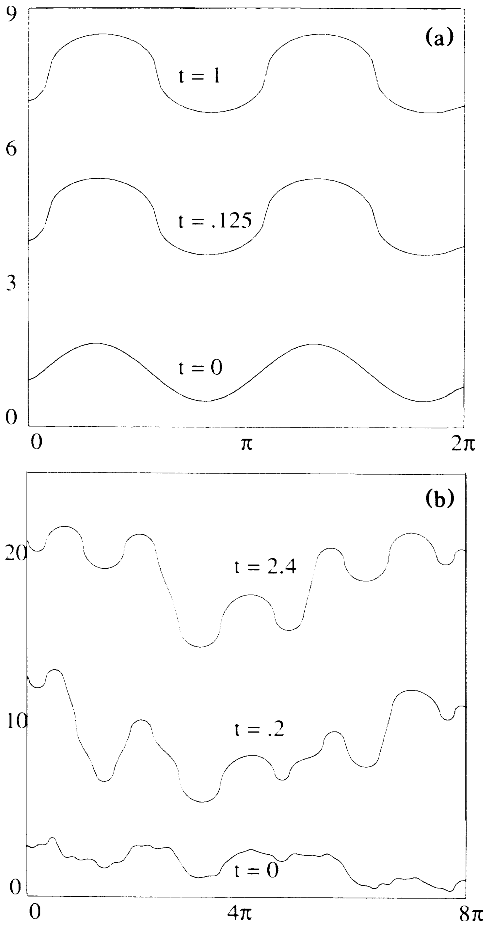

FIG. 2. Evolution of an initially (a) sinusoidal profile and (b) random profile, towards a stable steady state.

cally for both sinusoidal and random initial conditions [see Figs. 2(a) and 2(b)]. The profile evolves to steady solutions [given by (3) with $C > 0$] in between vertical slopes. Once the profile develops vertical slopes there is little additional evolution of the profile, and hence the profile can be irregular with no well-defined wavelength [see Fig. 2(b)]. For small initial perturbations of a flat substrate, however, the fastest growing wavelength λ_m tends to dominate the surface's evolution and set the wavelength of the final profile. Since λ_m is of the order of the wavelength of light (i.e., $\lambda_m \approx 10^{-4}$ cm to 10^{-5} cm for $T \approx 0.3T_m$ to $0.5T_m$), this roughness may be the cause of the matted surface finish typically observed in zone II.

The surface profile of a real film is modified by the presence of grain boundaries intersecting the growing surface and creating grooves with an opening angle $\cos(\Phi/2) = \sigma_{\text{gb}}/2\sigma_s$, where σ_{gb} is the grain-boundary energy density.[10] Numerically we find the surface profile between grain boundaries to evolve (rapidly) to a steady solution of (1). Specifically for grain sizes $d < \lambda_m$, the unique steady state consists of a smooth nearly circular cap connecting the grain boundaries [see Fig. 3(a)]. However, for d much above λ_m, diffusion is unable to smooth the surface over length scales of order d; consequently there are many steady states and a rough surface morphology occurs [see Fig. 3(b)].

Once steady states are attained between grain boundaries, the film can reduce its total energy only by coarsening the grain size. This coarsening process can only occur by translation of the grooves, and there are two mechanisms underlying it. The first is surface-curvature driven. For grain sizes $d < \lambda_m$, the net velocity across the groove and along the x axis is

$$v^x \propto -(\kappa^+ - \kappa^-)/\Delta x, \tag{4}$$

where κ^+ (κ^-) is the surface curvature at point x^+ (x^-) located at an infinitesimal distance Δx to the right (left) of the groove $x_g(t)$. The velocity of the groove can be written as $v_g = -v^x$ or as $v_g \propto d_t^{\mp}$, where $d^+ (d^-)$ are the grain sizes to the right (left) of the groove, and the subscript t implies differentiation with respect to time. The radius R^+ (R^-) of the circular surface cap of the grain d^+ (d^-) is given by $d^{\mp} = 2R^{\mp} \cos(\Phi/2)$. R^+ (R^-) is also inversely proportional to κ^+ (κ^-). Combining this information we find the mean grain size at the surface $\langle d \rangle$ to increase with time like

$$\langle d \rangle \approx \alpha t^{1,3}, \quad \alpha = \text{const}, \tag{5}$$

as long as $\langle d \rangle \leq \lambda_m$. However, for grain sizes much above λ_m this mechanism leads to little further coarsening since the surface profile simply moves into steady states which have equal curvature on both sides of the grain boundary.

Second, regardless of the surface curvature, the grain boundaries also move in response to grain-boundary curvature in the plane of the film. For this type of growth the mean grain size $\langle d \rangle$ at the surface grows asymptotically as[11]

$$\langle d \rangle \approx \beta t^{1/2}, \quad \beta = \text{const}. \tag{6}$$

Essentially all theories of growth driven by domain-wall curvature in nonconserved systems yield $t^{1/2}$ domain-growth kinetics. We expect that this $t^{1/2}$ growth law will dominate the $t^{1/3}$ law for all physically meaningful times.

Finally, we performed two-dimensional Monte Carlo simulations[5,12] of realistic three-dimensional zone-II microstructures. Specifically, we performed Monte Carlo simulations of the evolution of the surface microstructure on a triangular lattice with nonconserved order parameter (Glauber dynamics) at $T \approx 0$ following a quench from $T \gg T_c$ (the technique used is exactly that of Ref. 12). The Hamiltonian describing the system is that of a 48-fold degenerate Potts model which has been shown to reproduce experimental grain-growth microstructure accurately.[13] The correspondence between the two-dimensional simulation and film relies on the fact that for $T < 0.5T_m$ bulk diffusion is negligible relative to surface diffusion; thus the interior of the film is kinetically frozen and all microstructural development occurs at the free surface. Therefore, through-thickness cross section of the film may be represented by traces of the positions of grain boundaries in one of the two spatial dimensions plus the time dimension of the model. The simulations account for both growth competition between adjacent grains and the development of film texture due to surface energy anisotropy (i.e., a field that couples to certain orientations). Figure 4 shows a typical through-

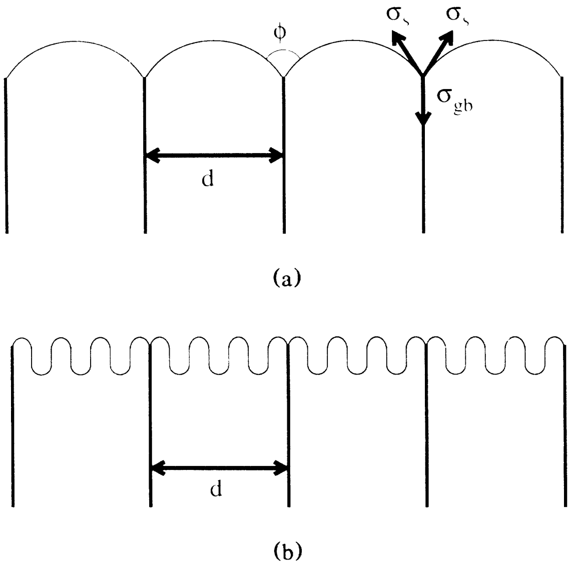

FIG. 3. (a) Smooth, nearly circular steady state between grain boundaries for $d < \lambda_m$. (b) Rough surface morphology attained for $d > \lambda_m$.

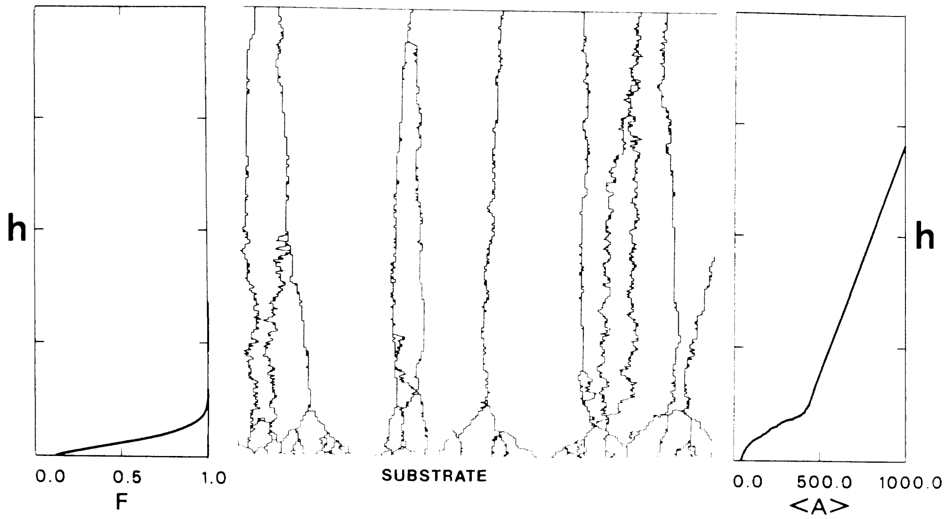

FIG. 4. Through-thickness cross section of a film from a Monte Carlo simulation. Initially, the fraction F of surface area covered by grains in the lowest-energy orientation was 0.10. Also shown are the mean grain area $\langle A\rangle$ and F as functions of film thickness (i.e., the vertical axis).

thickness cross section of a film in which initially 10% of the surface consisted of grains in the lowest surface energy orientation. This figure also shows the mean grain area $\langle A\rangle$ (in the plane of the film) and the fraction F of surface area in the lowest energy orientation as a function of film thickness (i.e., the vertical axis). As a result of the rapid growth of the low surface energy grains at the expense of the high energy ones, initially the microstructure exhibits a bimodal grain size distribution with $\langle A\rangle$ increasing quadratically and $\langle d\rangle$ increasing linearly with time. Once the surface is composed entirely of grains in the lowest energy orientation ($F=1$), further coarsening is controlled solely by the curvature of the grain boundaries. Consequently, the mean grain area $\langle A\rangle$ increases linearly in time, reflecting the growth law described in (6).

In conclusion, a theoretical model for the growth of zone-II microstructures has been presented. This model shows that the columnar growth is primarily controlled by competition between discrete atomic deposition and surface diffusion. The zone-I to zone-II transition temperature, the characteristic length scales associated with the unstable modes, the analytic steady-state surface morphology, the columnar grain structure, and the dependence of grain size on film thickness are all accounted for, in good agreement with experimental zone-II microstructures. Numerical simulations have substantiated this model and provided additional information about the development of columnar grains and film texture.

---

[1] B. A. Movchan and A. V. Demchishin, Phys. Met. Metallogr. **28**, 83 (1969).

[2] J. A. Thornton, Ann. Rev. Mater. Sci. **7**, 239 (1977).

[3] R. Messier, A. P. Giri, and R. A. Roy, J. Vac. Sci. Technol. A **2**, 500 (1984).

[4] R. F. Bunshah, J. Vac. Sci. Technol. A **11**, 814 (1974).

[5] D. J. Srolovitz, A. Mazor, P. S. Hagan, and B. G. Bukiet, to be published.

[6] H. J. Leamy, G. H. Gilmer, and A. G. Dirks, in *Current Topics in Materials Science*, edited by E. Kaldis (North-Holland, Amsterdam, 1980), Vol. 6, p. 309.

[7] W. W. Mullins, J. Appl. Phys. **28**, 333 (1957).

[8] K. H. Muller, J. Appl. Phys. **58**, 2573 (1985).

[9] J. S. Langer, Ann. Phys. (N.Y.) **65**, 53 (1971).

[10] G. L. J. Bailey and H. C. Watkins, Proc. Phys. Soc. B **63**, 350 (1950).

[11] S. M. Allen and J. W. Cahn, Acta Metall. **27**, 1085 (1979).

[12] D. J. Srolovitz, J. Vac. Sci. Technol. A **4**, 2925 (1986).

[13] P. S. Sahni, D. J. Srolovitz, G. S. Grest, M. P. Anderson, and S. A. Safran, Phys. Rev. B **28**, 2705 (1983).

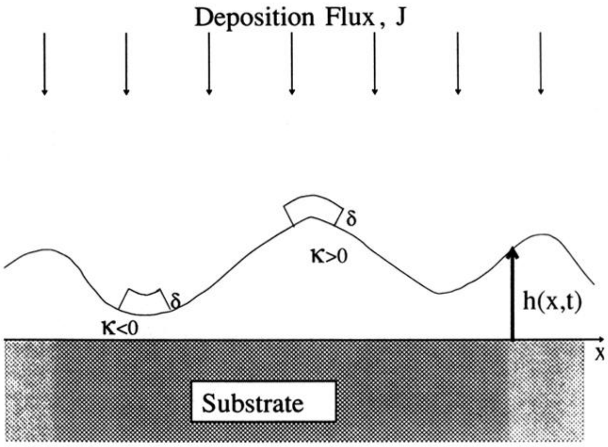
Deposition Flux, J
δ
κ>0
δ
κ<0
h(x,t)
x
Substrate

FIG. 1. The deposition geometry (κ is the surface curvature).